Bending Stiffness of Unsymmetrical Multilayered Corrugated Board: Influence of Boundary Conditions

Damian Mrówczyński,[a] Jolanta Pozorska,[b] Tomasz Garbowski,[c,*] and Zbigniew Pozorski [d]

In laboratory practice, several standards for testing the bending stiffness of corrugated board are used. There are often cases of tests where the results depend on the way the sample is placed on the supports. The problem arises when the board is five-ply (with two corrugated layers with different corrugation heights) or when the board has asymmetrically selected papers on the flat layers. This article focuses on the problem related to boundary conditions, with particular attention to the local effects of the support of the sample. Because the cardboard layers, both flat and corrugated, have a small thickness, a slight deformation of the papers can always be observed at the point of contact between the sample and the support, which affects the readings of the measured stiffness. The paper presents theoretical and numerical analyses showing how much the method of supporting the sample affects the measured bending stiffness of various samples. Numerical observations were compared with the results of analyses presented by other scientists as well as with experimental results.

DOI: 10.15376/biores.18.4.7611-7628

Keywords: Corrugated board; Bending stiffness; Multilayer unsymmetrical panels; Boundary conditions; Finite element analysis

Contact information: a: Doctoral School, Poznan University of Life Sciences, Wojska Polskiego 28, 60-637 Poznan, Poland; b: Department of Mathematics, Czestochowa University of Technology, Armii Krajowej 21, 42-201 Czestochowa, Poland; c: Department of Biosystems Engineering, Poznan University of Life Sciences, Wojska Polskiego 50, 60-627 Poznan, Poland; d: Institute of Structural Analysis, Poznan University of Technology, Piotrowo 5, 60-965 Poznan, Poland;
** Corresponding author: tomasz.garbowski@up.poznan.pl*

INTRODUCTION

Cardboard is a material commonly used around the world. The volume of production of cardboard products and the dynamics of the development make this sector in the first place of the entire paper industry. Cardboard is widely used mainly in the following industries: packaging, transportation, catering, construction and renovation, food, advertising, but also in everyday life.

Cardboard packaging is very common because it is a product that is cheap and suitable for mass production. Corrugated cardboard is made of paper, making it an environmentally friendly product and 100 percent recyclable, thus displacing plastic. Scientific research has shown that corrugated fibres can be reused more than 25 times without significant loss of quality (Putz and Schabel 2018), although heavy metal contamination of the cardboard is a problem (Mertoglu-Elmas 2017). It is also a very lightweight material. Hence, the packaging made of this material does not affect the final weight of the shipment. Ultimately, corrugated board is very strong, protects objects from

shock and mechanical damage, and absorbs impacts (Wang *et al*. 2021). Corrugated board composites are also ideal as elements of sound absorbers (Chanlert *et al.* 2022).

This product has a few disadvantages. Corrugated board is a material that is very sensitive to environmental conditions, especially moisture. It is also a material without special coatings or admixtures. Paper will not be resistant to moisture and needs proper storage and warehousing conditions. Moisture and temperature that is too high may cause a decrease in stiffness and cause stresses in the corrugated layers, which may lead to tearing of the paper. Moisture levels that are too low can lead to cracking of flutes in the corrugated layers in the material and, consequently, of entire cardboard sheets. The effect of temperature and relative humidity on the compressive strength of corrugated boxes is studied in Liu *et al.* (2010). The sensitivity of paperboard to environmental conditions is forcing manufacturers to seek new solutions such as innovative low-diffusion corrugated cardboard coated with a polymer-wax coating. An Innovative Cardboard ARchitecture Object, ICARO, modular, highly sustainable, has just been developed in Sicily and is in the testing phase (Sapienza *et al.* 2022).

Corrugated board is made by alternating layers of paper (liners and corrugated layers). The layers can have different thicknesses, and the flutes can have different geometries, *i.e.* different heights and lengths. The most commonly used flute types are: E, B, and C, with E being the lowest and C being the highest. Typically, 2-ply (cardboard), 3-ply and 5-ply corrugated cardboard are used. 7-layer and 9-layer boards are less frequently exploited. The 2-ply comes in rolls and is used to wrap items for protection during transportation. On the other hand, 3- and 5-layer corrugated boards are used for making packaging. 7- and 9-ply cardboards are intended for special tasks *e.g.* for bulk packaging. They are also used in the metallurgical and automotive industries.

The most important aspect of packaging is the appropriate protection of the goods during storage or transport. In order to assess the ability of the packaging to protect the goods, it is necessary to perform appropriate strength tests and determine the appropriate characteristics of the cardboard. The box compression test (BCT) is a test of the compression resistance of the finished, formed box (Marin *et al.* 2021). The packaging is compressed between two press plates, and the final BCT value is the maximum load-bearing capacity of the box. This method makes it possible to determine the maximum pressure that the finished box can withstand and the number of layers in which boxes with contents can be stored. The Edgewise Crush Test (ECT) determines the strength of corrugated board under edge pressure (Schrampfer *et al.* 1987; Bai *et al.* 2019), where the sample is placed on the press and compressed until strength is lost. The ECT is one of the most important cardboard parameters and is used to determine the strength of corrugated board packaging using analytical and analytical-numerical methods. The 4-point bending test expresses the resistance of multilayer paperboard to bending under the influence of forces acting perpendicular to its surface (Jamsari *et al.* 2019). The bending stiffness (BS) is defined per unit width of the element. The sample is placed on two cylindrical supports and then loaded using two more supports with a different spacing than the bottom supports. The test result is bending stiffness, which is also an important cardboard parameter on the basis of which the load-bearing capacity of the box can be analytically calculated. This test precisely indicates even small cardboard deformations that are impossible to determine by other methods. The stiffness indicates the crucial importance of board thickness and its influence on BCT.

Due to its great practical importance, the issue of determining the bending stiffness of cardboard (and not only) is constantly the subject of scientific publications. The

determination of bending properties of cardboard in three-point bending tests using samples of various span lengths was presented in Yoshihara *et al.* (2022). The bending stiffness and moment capacity per unit width were determined, and the effects of the testing method and span length were investigated. Of course, in the case of 3-point bending, shape deformations of the cardboard caused by shear forces should be taken into account. This issue may require an advanced approach (Buannic *et al.* 2003; Garbowski and Gajewski 2021). The problem of global or local loss of stability has also been discussed many times in the literature, mainly in the context of edge compression (Norstrand 2004; Popil 2012; Garbowski *et al.* 2020), and of course it does not apply only to cardboard (Åslund *et al.* 2014). However, the influence of the local deformation of the cardboard at the supports on the determination of its bending stiffness is omitted, although the significance of this phenomenon was presented in publications concerning, for example, sandwich panels (Błaszczuk and Pozorski 2012; Pozorska and Pozorski 2018). The flexural stiffness is also dependent on the moisture content, and this problem can be related to the stiffness of the pulp fibers (Lorbach *et al.* 2014).

Although traditional experimental methods are the basic and necessary tools for evaluating the properties of cardboard, they are often supported or supplemented by numerical analyses, which facilitates understanding the complexity of the observed phenomena and makes it possible to perform many simulations in a short time. Numerical analyses allow designers to test various solutions related to, for example, the selection of paper layers and checking the impact of these changes on the cardboard parameters without the need to produce actual cardboard with a changed set of papers. This possibility significantly speeds up the process of searching for the optimal cardboard composition that meets customer requirements. In Urbanik and Frank (2006), FEM and data obtained from multiple literature sources were used to derive a more general box compression formula. FEM was also applied to observe buckling phenomena of corrugated cardboard boxes (Urbanik and Saliklis 2003). In Sohrabpour and Hellström (2011), numerical models were used to predict cardboard properties and corrugated box properties. Extensive discussion on the topic of numerical strength estimation of corrugated board packages can be found in Park *et al.* (2020).

This study discusses the 4-point bending test and the influence of local cardboard deformations on the obtained value of bending stiffness. This problem, overlooked in the literature, is extremely important. The correct assessment of the properties of the cardboard is of great importance for the prediction of the functional properties of cardboard packaging. The main purpose of the work is the numerical analysis of the influence of the arrangement of the sample on the supports on the determined bending stiffness for many types of asymmetric corrugated board.

EXPERIMENTAL

The Four-Point Bending Test of Asymmetric Corrugated Board

Test procedure

The 4-point bend test is the most common test used to determine the bending stiffness of various materials, including corrugated board. It consists of bending a sample placed on two bottom supports, by moving two upper supports, which have a spacing greater than the lower supports. The test scheme is shown in Fig. 1. Such arrangement of supports allows for pure bending, which means that in the part of the sample between the

bottom supports there is a constant bending moment without the simultaneous action of other cross-sectional forces. Bending stiffness per unit width can be calculated as follows (PN-EN ISO 5628 1990),

$$BS = \frac{FL_1{L_2}^2}{8db} \quad (1)$$

where BS is the bending stiffness (Nmm), F is the force (N), L_1 is the distance between the outer support and its nearer inner support (mm), L_2 is the distance between the inner supports (mm), d is the deflection of the sample center (mm), and b is the test sample width (mm).

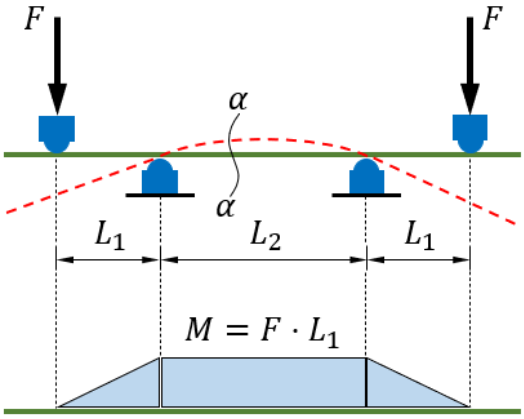

Fig. 1. Static scheme of the 4-point bending test

Asymmetry and sample positions

In the middle part of the cardboard sample L_2, the sample is subjected to bending with a constant moment FL_1, *i.e.* the upper part of the cross-section is stretched while the bottom part is compressed. Testing corrugated board with an asymmetric cross-section, measurements should be taken for two positions of the sample, as shown in Fig. 2. In the first position of the sample (Fig. 2a), the higher flute part of the sample is compressed, and the lower flute side is stretched. For this configuration, lower bending stiffness values are usually obtained compared to the results obtained from bending the same sample but arranged in the opposite way (Czechowski *et al*. 2021; Garbowski and Knitter 2022), see Fig. 2b. For this reason, it can be assumed that the side of the cross-section with the higher flute (B in this example) is "weaker" and the part with the lower flute (E in this example) is "stronger".

Notation of cardboard types

To distinguish between the two positions of the sample during the test, the name of cardboard was described with two letters denoting the type of flute. The letter corresponding to the stretched flute was written first (in Fig. 2, the upper flutes are stretched), and the letter related to the compressed flute - second (in Fig. 2, the bottom flutes are compressed). In practice, one can find many asymmetric corrugated boards, these will be all double-walled (*i.e.* 5-layer) cardboards with two different flutes, starting from the most common EB, through BC to less known EC and many others.

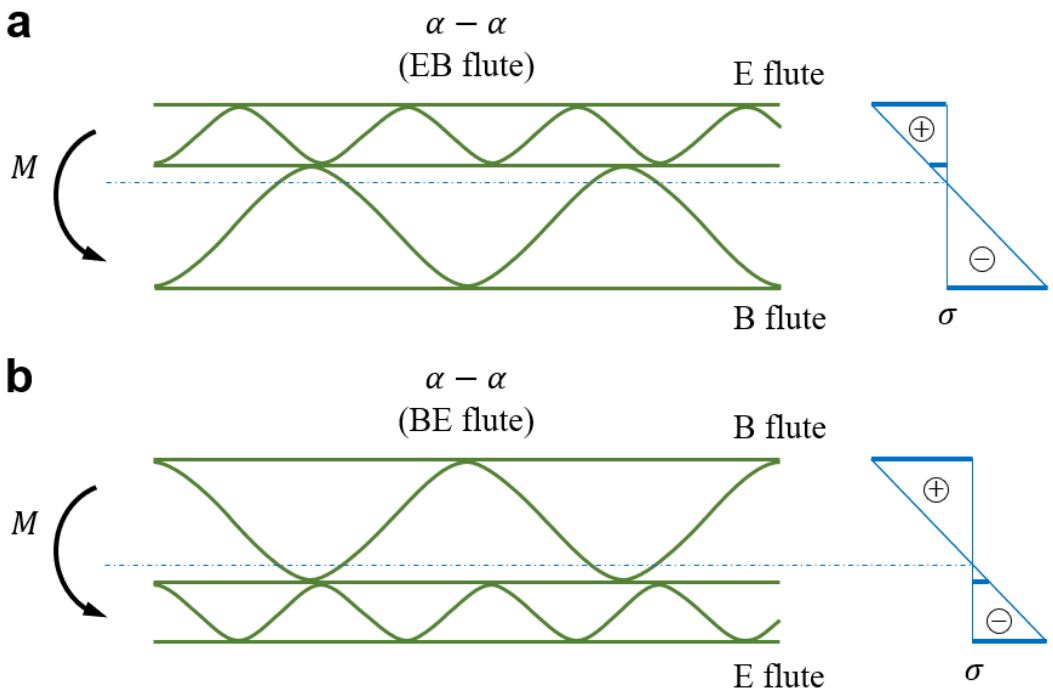

Fig. 2. Two possible positions of the cardboard sample in the 4-point bending test: (a) B flute downwards (EB flute) and (b) E flute downwards (BE flute).

In the case of the above-mentioned double-walled corrugated boards, the notation EB, EC, and BC means the compression of the section with the "weaker" higher flute (case **a** in Fig. 2), and the notation BE, CE, and CB means the compression of the part with the "stronger" lower flute (see case **b** in Fig. 2). An asymmetric cross-section can also be obtained for five-layer cardboard with two of the same flutes and for three-layer cardboard but only if different papers for the external flat layers are used, as shown in Fig. 3. In such cases, the position of the sample with the stronger liner in tension will be indicated by letters corresponding to the flute types (EE, B, and C) (see cases **a** and **b** in Fig. 3), and the position with the stronger liner in compression will be written with the subscript "rev" (EE_{rev}, B_{rev}, C_{rev}), see cases **c** and **d** in Fig. 3.

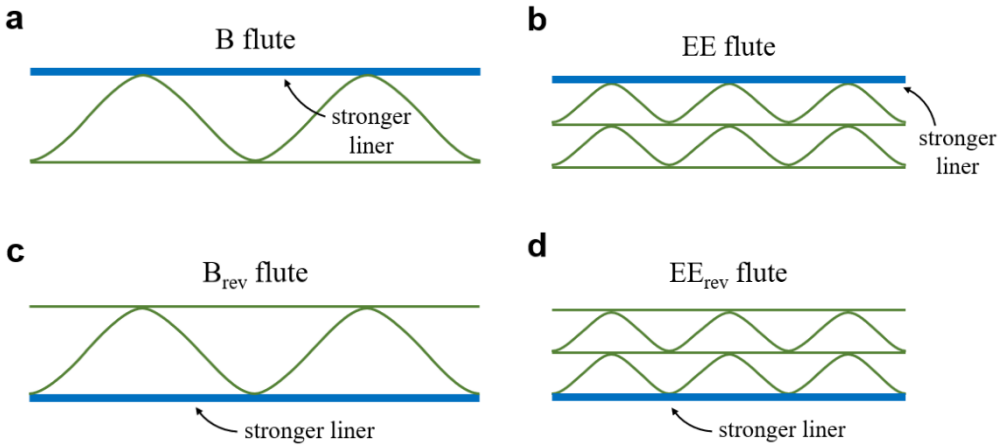

Fig. 3. Possible positions of single-walled cardboard and double-walled cardboard with two the same flutes: (a) B flute – tension of stronger liner, (b) EE flute – tension of stronger liner, (c) B_{rev} flute – compression of stronger liner and (d) EE_{rev} flute – compression of stronger liner

Corrugated Board – Geometry and Materials

Geometry of corrugated cardboard

Corrugated board is a material consisting of flat layers (liners) and corrugated layers (flutings) connected with each other by an adhesive joint in the production process. The geometry of the cardboard is mainly determined by the corrugated layers, which have a sinusoidal shape. Therefore, they can be described by two values: the wavelength p and the height h of the flute. In Fig. 4, a simplified geometry scheme of double-walled corrugated board is shown, where p_i is the wavelength of the i-th flute and h_i is the height of the i-th flute. In Table 1, the geometrical parameters of the flutes used in the analyses are presented.

Table 1. Geometry Data of Corrugated Cardboard Flutes

Flute	Wavelength (mm)	Height (mm)
B	6.5	2.46
C	8.0	3.61
E	3.5	1.15

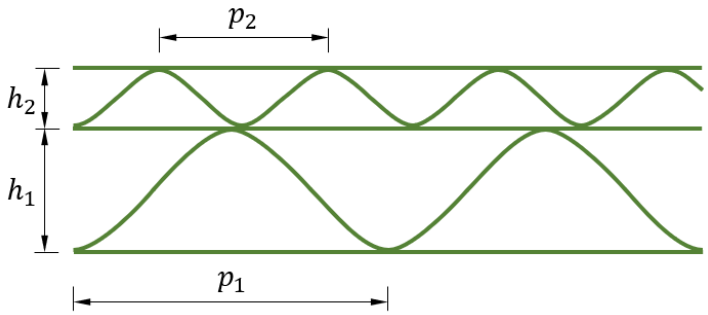

Fig. 4. Geometry of the double-walled corrugated cardboard flutes, where $\boldsymbol{p_1}$ and $\boldsymbol{h_1}$ are the period and height of the bottom flute, respectively, and $\boldsymbol{p_2}$ and $\boldsymbol{h_2}$ are the period and height of the upper flute, respectively.

Incorporating layer thickness

In Fig. 4, a simplified geometric scheme of a double-walled cardboard is shown, which does not take into account the thickness of the layers. Since the bending stiffness, apart from the fluting geometry, also significantly depends on the thickness of the corrugated board layers, the actual location of the central axis of each layer was used in the numerical model. Unfortunately, this approach results in some gaps between the layers represented by the central axes in the model. In Fig. 5, a cross-section of the five-layer corrugated board with paper layer thicknesses is presented.

Taking into account the thickness of the layers allowed to determine the actual axial distance between the liners,

$$h_1' = h_1 + 0.5t_1 + t_2 + 0.5t_3, \quad (2a)$$

$$h_2' = h_2 + 0.5t_3 + t_4 + 0.5t_5, \quad (2b)$$

where h_i' is the distance between the central axes of the liners. Based on the above equations and Fig. 5, the total height of the five-layer cardboard can be represented as,

$$H = 0.5t_1 + h_1' + h_2' + 0.5t_5 \quad (3)$$

and the total height of the three-layer cardboard as:

$$H = 0.5t_1 + h_1' + 0.5t_3. \quad (4)$$

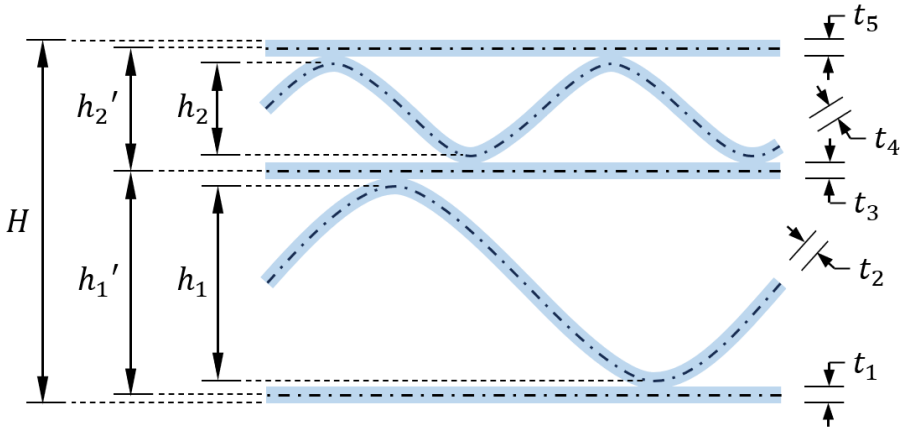

Fig. 5. The geometry of the numerical model

Material properties

Corrugated board is an orthotropic material; however, considering bending stiffness only in the machine direction, the paper layers can be modeled as an isotropic material. Therefore, just Young's modulus, Poisson's ratio and layer thickness are used in 2D modeling. In Table 2, thickness and material parameters for each paperboard layer of various cardboard analyzed here are presented.

Table 2. Corrugated Board Data

Corrugated Cardboard	Layer	Thickness (mm)	Young's Modulus (MPa)	Poisson's Ratio (–)
B and C	1	0.195	5427	0.483
	2	0.185	5538	0.484
	3	0.259	5684	0.484
EE	1	0.188	5113	0.442
	2	0.156	5479	0.468
	3	0.130	5358	0.414
	4	0.156	5479	0.468
	5	0.259	5684	0.484
EB and EC	1	0.180	4906	0.427
	2	0.142	5327	0.464
	3	0.130	5358	0.414
	4	0.156	5479	0.468
	5	0.188	5113	0.442
BC	1	0.255	6016	0.456
	2	0.197	5652	0.500
	3	0.126	5548	0.432
	4	0.202	5680	0.497
	5	0.260	5458	0.450

Boundary Conditions in the Four-Point Bending Test – Numerical Study

Model setup

The 4-point bending test of the corrugated board was simulated in finite element method (FEM) software (Simulia ABAQUS FEA, commercial version 2020). According to the scheme shown in Fig. 1, the cardboard sample was placed on the bottom supports and loaded with the upper supports. The distance between the upper support and the nearest

bottom support L_1 was 50 mm, and the distance between the bottom supports L_2 was 100 mm. The total length of the sample was 250 mm and the width of sample b was equal to 50 mm.

Because in this study the bending stiffness was considered only in the machine direction, the simplified 2D modeling was used. In other words, the cross-sections of the corrugated board (each paperboard layer) were modeled using two node Timoshenko beam elements. The beam elements were assigned a rectangular cross-section with a width of b equal to 50 mm and a height of t in accordance with the values given in Table 2. It was necessary to shift the individual cardboard layers by appropriate distances resulting from the assigned layer thicknesses. Such a treatment was necessary to achieve the appropriate moment of inertia of the cardboard. In Fig. 6, the numerical model of the cardboard without and with the visualization of the assigned layer thickness is shown.

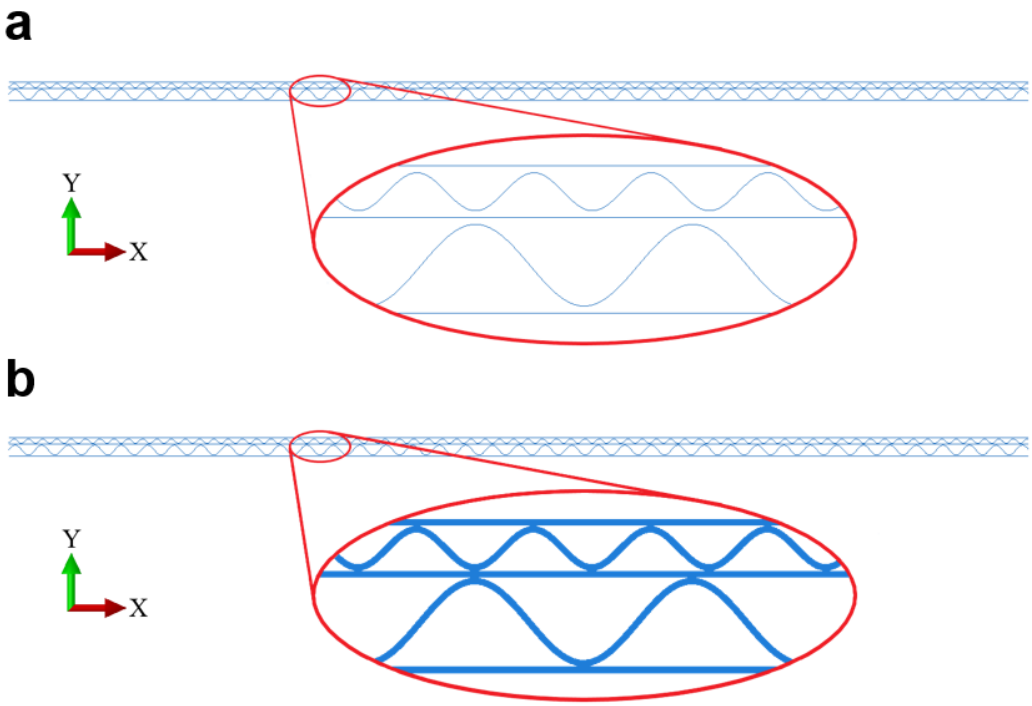

Fig. 6. Numerical cardboard model: (a) without thickness visualization and (b) with thickness visualization.

Consistent behavior of the flat and corrugated layers was obtained by using a "tie" technique, which ensures the structure integrity (continuity of displacement) between the crests of the flutes and the flat layers (Fig. 7). The material of the cardboard layers was modeled as isotropic and linearly elastic. Table 2 presents the respective material parameters.

The 4-point bending test was modeled according to the scheme shown in Fig. 1. Vertical displacements were blocked on the lower supports, and vertical displacements were allowed in the places of the upper supports. To ensure the correct bending behavior of the cardboard, the horizontal displacement of the liners was blocked in the middle of the sample length.

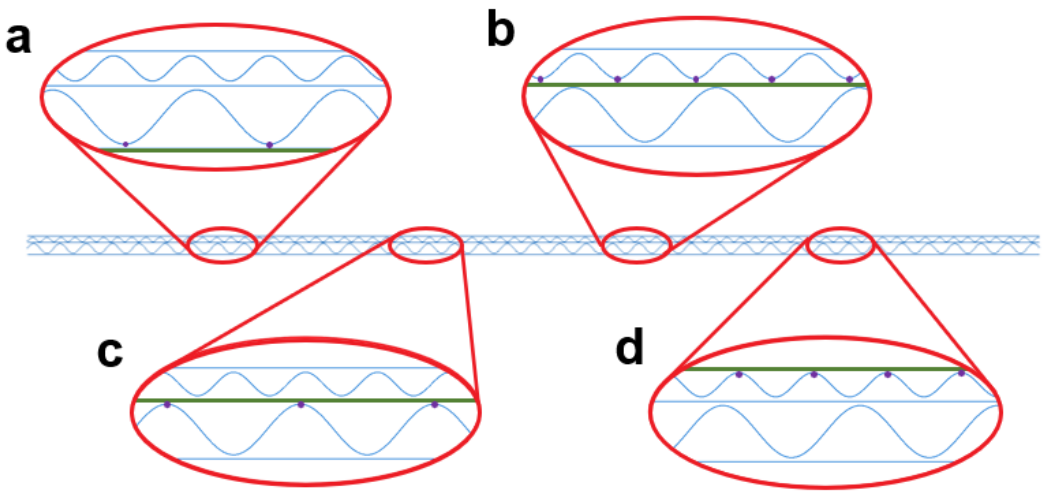

Fig. 7. Visualization of the structure integrity between: (a) the bottom liner and the crests of the bottom flute, (b) the middle liner and the crests of the upper flute, (c) the middle liner and the crests of the bottom flute and (d) the upper liner and the crests of the upper flute

Analysis variants

Simulations of the 4-point bending test were performed for four types of five-layer cardboard (EB, EC, BC, and EE flutes) and two types of three-layer cardboard (B and C flutes). The samples were loaded in two configurations: the "stronger" part of the cross-section upwards and downwards. In order to assess the influence of the location of the sample on the supports, the shift of the flute crest relative to the support was changed. In double-walled corrugated boards, both the bottom flute relative to the bottom support and the upper flute relative to the upper support were shifted independently. The shift value ranged from 0% to 90% in increments of 10%. In this way, a full spectrum of bending stiffness was obtained depending on the location of the flute crest relative to the support. In a single-walled cardboard there is only one flute, so it was shifted first relative to the bottom and then relative to the upper support.

The setup of the 4-point bending test is obviously symmetrical with respect to the vertical axis. However, the cardboard sample in this test is no longer symmetrical. This is due to the fact that the location of the crest of the flute in relation to the left support will be in general different than in relation to the right support. Therefore, the flute shift was determined in relation to the bottom and upper supports on the left side of the model. The shift of the flute was recorded as a percentage and determined by a percentage shift of the flute's crest relative to the support. For example, a flute shift of 0% means that the flute crest is at the support, and a 25% shift means that the flute crest is shifted 25% of the wavelength to the right. Figure 8 shows several variants of shifts for five-layer cardboard.

Based on all the described variants, each selected test variant can be marked with the symbol X-Y-zz for three-layer cardboard and XX-yy-zz for five-layer cardboard. For single-walled corrugated board, X means the flute type as described in the Experimental section (B, B_{rev}, C or C_{rev}). Symbol Y indicates the support on which the shift occurs. In this case, two options are possible: B – bottom support and U – upper support. The number zz denotes the value of the flute crest shift relative to the Y support. For example, the B_{rev}-U-20 means three-layer B-flute cardboard with a stronger liner compressed and with a shift of the flute crest relative to the upper support by 20% of the wavelength. For double-walled cardboard, XX denotes the flute type (EB, BE, EC, CE, BC, CB, EE or EE_{rev}). The numbers

yy and zz mean the shift values of the bottom and upper flutes relative to the bottom and upper supports, respectively. The numbers yy and zz for five-layer cardboard and zz for three-layer cardboard can be 00, 10, 20, 30, 40, 50, 60, 70, 80 or 90. For example, EB-40-00 means five-layer cardboard with E and B flutes, where the B flute is compressed (the lower part of the sample) and the E flute is stretched (the upper part of the sample). Additionally, the shift of the lower flute crest relative to the lower support is 40% of the lower flute period and the upper flute crest is not shifted relative to the upper support (0% shift). Using a symbolic notation system, the variants shown in Fig. 8 can be represented as (a) EB-00-00 and (b) EB-30-60.

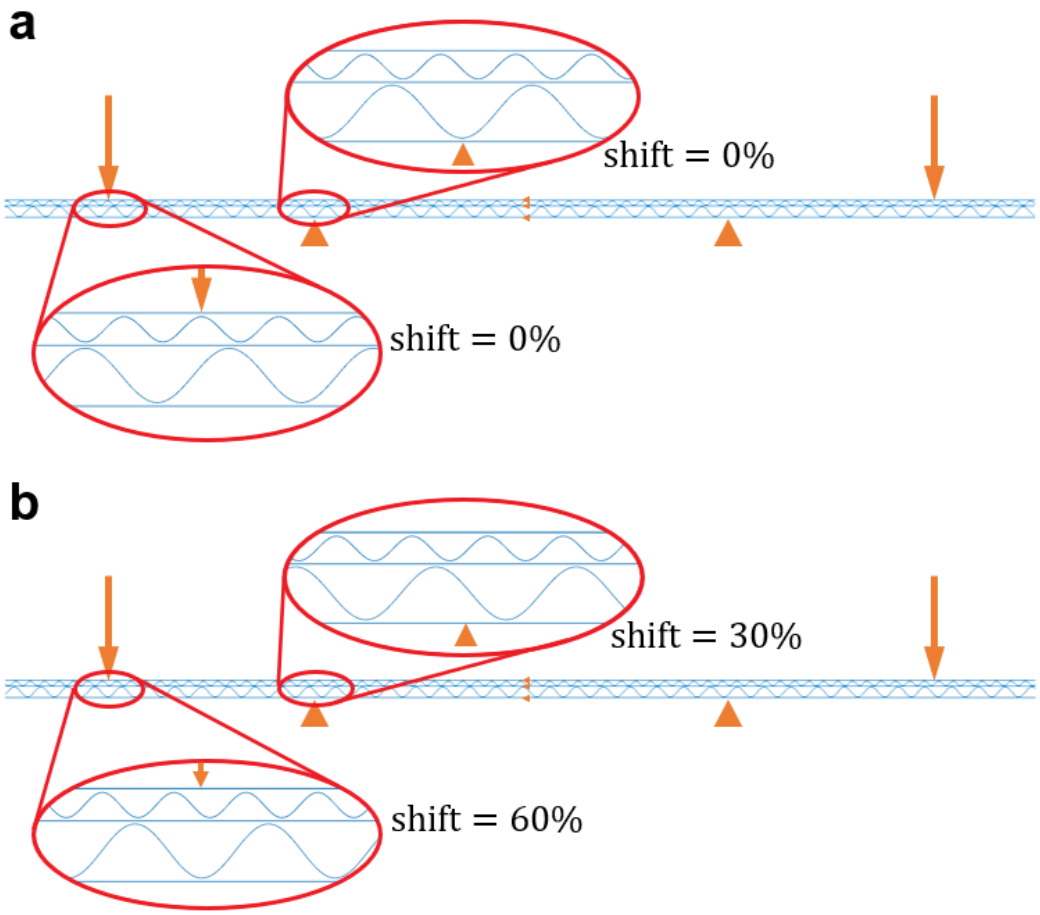

Fig. 8. The shifts of the flute crests relative to the supports for the model: (a) EB-00-00 and (b) EB-30-60.

Finite element analysis

In all analyses, the two-node planar linear beam elements (B21 elements) were used (This product has few disadvantages. FEA Software). All models were generated in FEM commercial software. From the analyses performed, the reactions in all supports and the vertical displacement of the sample center were obtained, which are necessary to calculate the bending stiffness in accordance with Eq. (1). An approximate global finite element length of 0.2 mm was assumed. Various types of cardboard were analyzed, therefore the number of elements for each model was different. For example, in the case of EB-00-00, the numerical model consists of 6,569 nodes, 6,564 elements and 19,707 degrees of freedom.

RESULTS AND DISCUSSION

Preliminary Observations

Figure 9 shows left supports (lower and upper) in two sample arrangements: (a) BC with lower and upper flutings shifted by 50%; (b) CB with the same shift of both wavy layers. In both Fig. 9a and 9b, the displacements shown are scaled to emphasize the local deformations at both supports. The colors in the figures indicate the stress concentration. Here the reduced Huber-Mises-Hencky stresses are shown. It is clear from these graphs that the influence of the boundary conditions of the corrugated board samples in the 4-point bending test on the global behavior of the sample is evident.

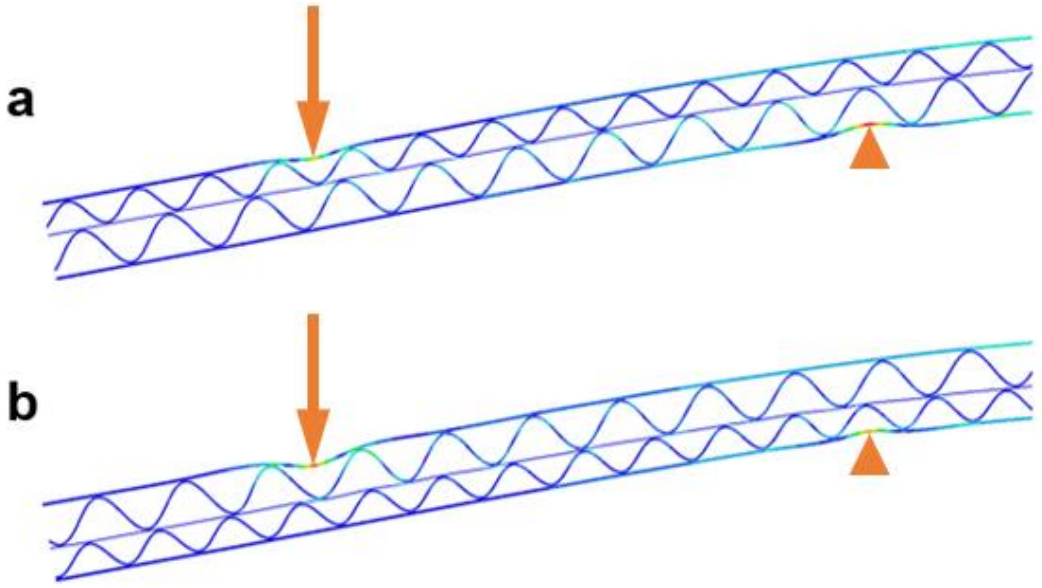

Fig. 9. Scaled displacements and the Huber-Mises-Hencky equivalent stress map on left supports for the two samples: (a) BC-50-50 and (b) CB-50-50

The purpose of this work, however, was not to indicate that the influence of supports on bending stiffness is evident, but rather to try to quantify it. The same principles of loading and flutes shifting as described in the previous section were maintained in all numerical analyses. In all calculated examples, the applied displacement on the upper support was only 0.2 mm in order to avoid the need to use non-linear geometrical analysis.

Because it seemed obvious that the location of the flute tops of the corrugated layers relative to the supports would have the greatest impact on the bending stiffness, this issue was given the most attention. Because the modeling of the shifts of the corrugated layers was already described in detail in the previous section, only the problem of averaging the results on supports will be explained here.

In all analyzed cases, it was assumed that the lower supports are stationary and that the crest of the lower flute can fall exactly on the support or at a certain distance from it. However, the position of the flute relative to the support can only be determined relative to one of the supports – in this case the left one. That means that the position of the flute on the second support, the right one, is rather accidental. The same also applies to the upper supports, where the position of the upper fluting was controlled only on the left support. Thus, on the right support the crest of the flute appeared in a random location relative to

the support (*i.e.* the position of the flute crest resulted from the wavelength and the distance between the supports). Therefore, in order to correctly and fairly indicate the influence of the position of the fluting relative to the supports on the bending stiffness of the cardboard samples, the reactions at both lower supports were averaged. These averaged reactions were then used to calculate the bending stiffness from Eq. 1. The same could of course also be done on the upper supports, but due to the balance of forces in the model, both results would be identical. Thus, the procedure for quantifying the influence of the position of the fluting vertices relative to the supports in the 4-point bending test was as follows: (i) in each numerical analysis, three matrices are generated: L_{ij} (reactions in the lower left support), R_{ij} (reactions in the lower right support) and d_{ij} (vertical displacements in the center of the sample span), where the index *i* controls the position of the flute relative to the lower left support and the index *j* controls the position of the fluting relative to the upper left support; (ii) average reaction is computed from R_{ij} and L_{ij}; (iii) bending stiffness is computed using Eq. (1); (iv) a statistical analysis of differences in bending stiffness is performed for each fluting position relative to the bottom left support.

Table 3. Bending Stiffness of all Cardboards in Both Arrangements

Corrugated Board	Bending Stiffness (Nmm)			
	Mean value	Standard deviation	Minimum	Maximum
B	5158	16.8	5133	5187
B_{rev}	5210	32.3	5167	5260
BC	38,174	876.9	36,657	39,923
CB	40,672	1004.5	38,904	42,492
BE	8868	152.8	8701	9192
EB	8490	18.3	8448	8527
C	10,395	33.9	10,347	10,441
C_{rev}	10,802	108.7	10,656	10,955
CE	16,364	516.0	15,634	17,004
EC	14,056	22.1	14,010	14,100
EE	5225	2.3	5220	5229
EE_{rev}	5245	3.7	5237	5252

Table 3 presents all computed bending stiffnesses for all samples in both arrangements. Figures 10 through 15 present the statistical distributions of the differences between the calculated bending stiffness in two different positions of the sample on the supports for six cardboards: (a) B *vs.* B_{rev} (see Fig. 10); (b) BE *vs.* EB (see Fig. 11); (c) C *vs.* C_{rev} (see Fig. 12); (d) CB *vs.* BC (see Fig. 13); (e) CE *vs.* EC (see Fig. 14), and (f) EE *vs.* EE_{rev} (see Fig. 15). Blue boxes on each figure indicate 25^{th} to 75^{th} percentiles of the data, while the central red line indicates the median. The whiskers extend to the most extreme data points not considered outliers, and the outliers are plotted individually using the '+' marker symbol.

Detailed Analysis of Various Cases

Figure 10 shows very clearly that the bending stiffness measured in the 4-point bending test varies depending on how the sample is placed in the machine, *i.e.* stronger side up or weaker side up. The mean values of bending stiffness differences depend on the position of the fluting relative to the bottom support range from 0.65 to 1.40 percent. The

minimum difference in this case was 0.58% while the maximum was 1.61%. The average difference in bending stiffness of all cases was 1.00±0.32%.

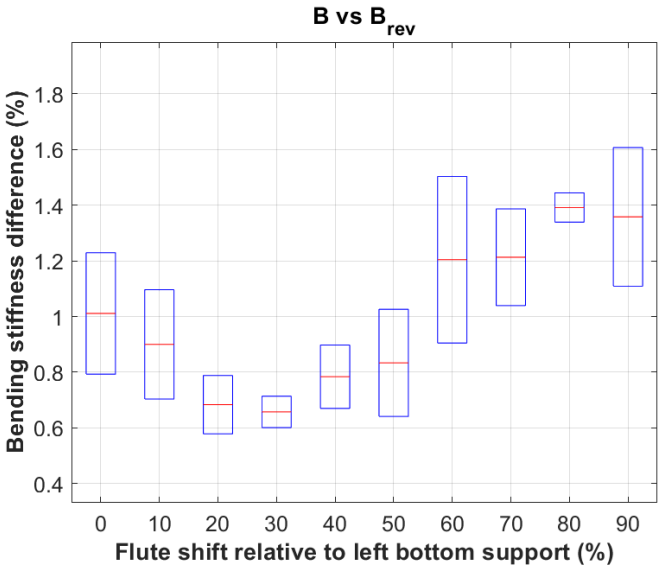

Fig. 10. Percentage difference in bending stiffness for cardboard example B and B_{rev}

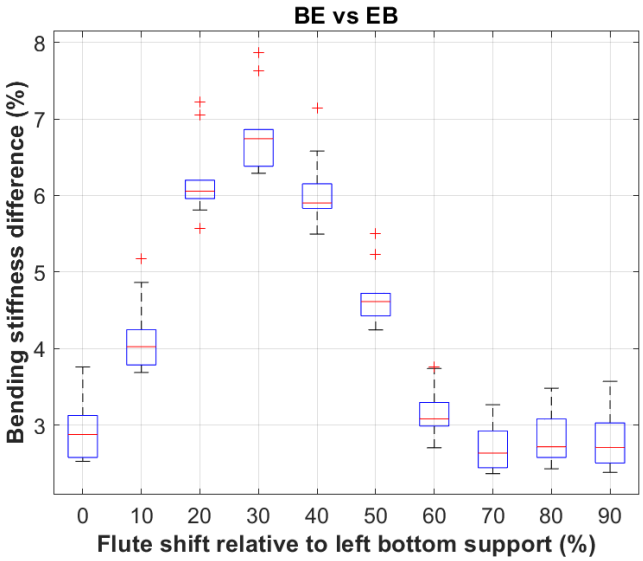

Fig. 11. Percentage difference in bending stiffness for cardboard example BE and EB

In the case of BE and EB boards, this difference was found to be much more pronounced (see Fig. 11) than in the previous case (see Fig. 10), where the only source of asymmetry was the difference in stiffness of the outer liners. In the case of BE and EB board, the asymmetry resulted from the difference in the geometry of the corrugated layers on the two sides of the sample. The minimum difference was 2.36%, the maximum was 7.87%, and the average difference of all cases was 4.25±1.59%.

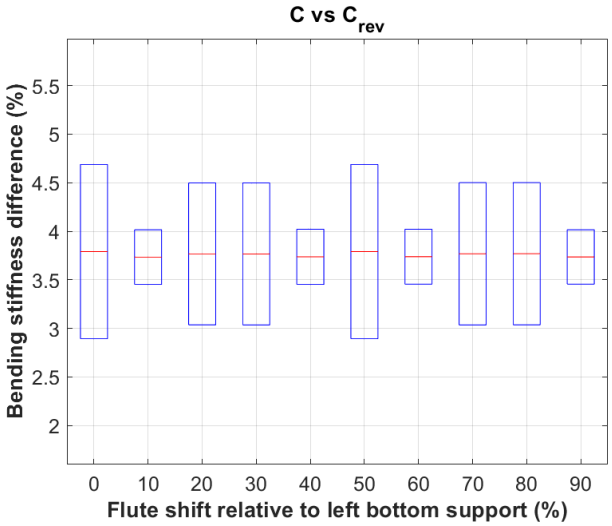

Fig. 12. Percentage difference in bending stiffness for cardboard example C and C_{rev}.

Figure 12 shows the discrepancy between bending stiffness of two different corrugated boards (*i.e.*, different in the sense of placing the sample in the slot of the 4-point bending test with the stronger side up or down). In the case of C and C_{rev} board, the average difference in bending stiffness of all cases was 3.76±0.65%. Minimum bending stiffness difference in this case was 2.89% while the maximum value was 4.69%.

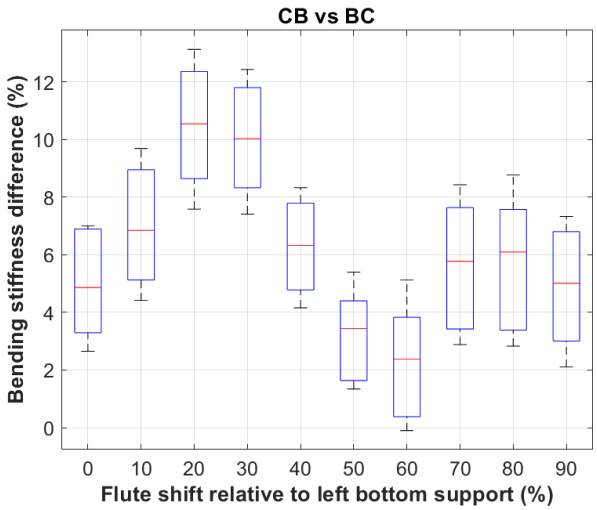

Fig. 13. Percentage difference in bending stiffness for cardboard example CB and BC

Figure 13 shows that the higher the flutes of the corrugated layer that are used in the corrugated board, the greater the differences in bending stiffness. In fact, in one case (for the fluting shift relative to the lower left support by 60%), the minimum bending stiffness difference was 0%, but the maximum difference in another case was as much as 13.13%. There was also a clear and characteristic wavy trend of the bending stiffness difference depending on the position of the fluting relative to the bottom left support. In the case of CB and BC board, the average difference in bending stiffness of all cases was nearly 6.09±3.06%.

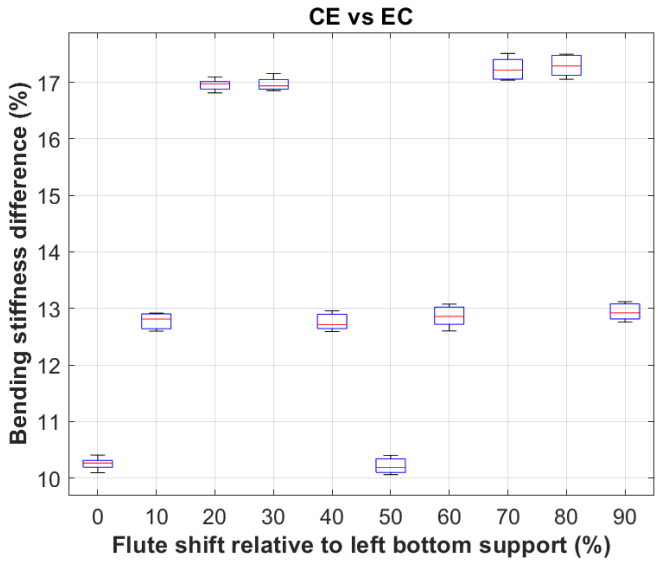

Fig. 14. Percentage difference in bending stiffness for cardboard example CE and EC

The case of CE and EC board (shown in Fig. 14) is special because the difference between the lower flute and the higher flute is the largest, which also results in the largest discrepancy between the bending stiffnesses of CE and EC board. The minimum bending stiffness difference was 10.06% and the maximum was 17.51%. The average discrepancy of all possible configurations of the positions of both flutings in relation to the bottom and top supports was slightly more than $14.02 \pm 2.71\%$.

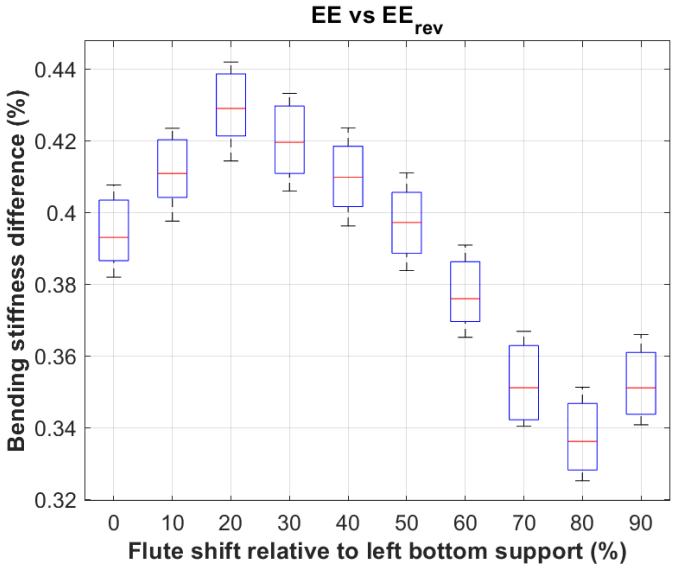

Fig. 15. Percentage difference in bending stiffness for cardboard example EE and EE_{rev}

The difference in bending stiffness in the case of EE and EE_{rev} board was the least clear (see Fig. 15), as it ranged from 0.32% to 0.44%. Such small percentage differences in bending stiffness result from small wavelength of fluting E. The paper of the liners stretched between the densely arranged tops of the flutes does not undergo such large local

deformations as in the case of higher flutes, which of course has a positive effect on the stability of the measurable stiffness in the 4-point bending test.

Important Observations

All of the above observations lead to the unequivocal conclusion that the stiffness of the corrugated board in the 4-point bending test depends on how the sample is placed in the machine. This is very clear, especially when the cardboard is asymmetrical due to the use of two different flute lengths in 5-layer cardboard or liners with different stiffness in the case of 3-layer cardboard. Bending stiffness is higher when the stronger side of the corrugated board is compressed, and lower when the weaker side of the corrugated board is compressed. These observations are in line with those found in the literature. For example, Czechowski *et al*. (2021) experimentally demonstrated such relationships for many different cases of cardboard. Although the authors did not indicate the reasons for these differences during the conducted research, the experimental data from the 4-point bending test are unambiguously consistent with those indicated in this work. In another paper (Garbowski and Knitter 2022), the authors explain the difference between the bending stiffness of asymmetric samples of various cardboards with imperfection that activates the buckling of compressed flat layers of corrugated boards during bending. The authors found some correlation between the proposed models and the available experimental data; however, the predictions of the model in several cases were not very precise. Perhaps if the effects of imperfections and boundary conditions were combined, the predictive models would be more accurate.

CONCLUSIONS

1. A very clear difference was found between the bending stiffness of the unsymmetrical corrugated board samples which differ only in the way they are arranged, *i.e.* those in which weaker or stronger layers are compressed during the 4-point bending test.
2. The difference in bending stiffness is greater in the case of cardboards with more pronounced asymmetry, *i.e*., when two very different flutes of corrugated layers are used.
3. The bending stiffness difference results, among others, from the position of the flute crests of the corrugated layers relative to the supports. The further the crest is from the support, the more pronounced the local bending effects of the flat layers, which obviously leads to greater differences in bending stiffness.
4. In this type of 4-point bending test, there is no way to avoid the formation of local disturbances that affect the estimated bending stiffness, unless a different support design is used. Therefore, it is important to understand the origin of bending stiffness differences when examining corrugated board, especially when it is characterized by very high asymmetry.

The conclusions of this article allow for a better understanding of the mechanics and behavior of corrugated cardboard during bending. This information can be used mainly by designers and manufacturers of asymmetric cardboard packaging for optimal, rational, and conscious design of boxes in terms of load-bearing capacity.

REFERENCES CITED

Abaqus Unified FEA Software. Available online: https://www.3ds.com/products-services/simulia/products/abaqus (accessed on 15 July 2023).

Åslund, P. E., Hägglund, R., Carlsson, L. A., and Isaksson, P. I. (2014). "Modeling of global and local buckling of corrugated board panels loaded in edge-to-edge compression," *Journal of Sandwich Structures & Materials* 16(3), 272-292. DOI: 10.1177/1099636213519374

Bai, J., Wang, J., Pan, L., Lu, L., and Lu, G. (2019). "Quasi-static axial crushing of single wall corrugated paperboard," *Compos. Struct.* 226, article 111237. DOI: 10.1016/j.compstruct.2019.111237

Błaszczuk, J., and Pozorski, Z. (2012). "The analysis of the influence of core compression effect on the determination of the shear modulus of sandwich panel core," *Scientific Research of the Institute of Mathematics and Computer* 11(2), 5-13. DOI: 10.17512/jamcm.2012.2.01

Buannic, N., Cartraud, P., and Quesnel, T. (2003). "Homogenization of corrugated core sandwich panels," *Comp. Struct.* 59(3), 299-312. DOI: 10.1016/S0263-8223(02)00246-5

Chanlert, P., Jintara, A., and Manoma, W. (2022). "Comparison of the sound absorption properties of acoustic absorbers made from used copy paper and corrugated board," *BioResources* 17(4), 5612-5621. DOI: 10.15376/biores.17.4.5612-5621

Czechowski, L., Kmita-Fudalej, G., Szewczyk, W., Gralewski, J., and Bieńkowska, M. (2021). "Numerical and experimental study of five-layer non-symmetrical paperboard panel stiffness," *Materials* 14, article 7453. DOI: 10.3390/ma14237453

EN ISO 5628 (1990). "Paper and board — Determination of bending stiffness by static methods — General principles," European Committee for Standardization, Brussels, Belgium.

Garbowski, T., Gajewski, T., and Grabski, J. K. (2020). "The role of buckling in the estimation of compressive strength of corrugated cardboard boxes," *Materials* 13(20), article 4578. DOI: 10.3390/ma13204578

Garbowski, T., and Gajewski, T. (2021). "Determination of transverse shear stiffness of sandwich panels with a corrugated core by numerical homogenization," *Materials* 14, 1976. DOI: 10.3390/ ma14081976

Garbowski, T., and Knitter-Piątkowska, A. (2022). "Analytical determination of the bending stiffness of a five-layer corrugated cardboard with imperfections," *Materials* 15(2), article 663. DOI: 10.3390/ma15020663

Jamsari, M. A., Kueh, C., Gray-Stuart, E. M., Dahm, K., and Bronlund, J. E. (2019). "Experimental and numerical performance of corrugated fibreboard at different orientations under four-point bending test," *Packag. Technol. Sci.* 32, 555-565. DOI: 10.1002/pts.2471

Liu, M., Yang, C., and Wang, H. J. (2010). "Effects of the temperature and relative humidity on the compression strength of corrugated cardboard boxes," in: *Proceedings of the 17th IAPRI World Conference*, pp. 136-139.

Lorbach, C., Fischer, W. J., Gregorova, A., Hirn, U., and Bauer, W. (2014). "Pulp fiber bending stiffness in wet and dry state measured from moment of inertia and modulus of elasticity," *BioResources* 9(3), 5511-5528. DOI: 10.15376/biores.9.3.5511-5528

Marin, G., Srinivasa, P., Nygårds, M., and Östlund, S. (2021). "Experimental and finite element simulated box compression tests on paperboard packages at different moisture levels," *Packag. Technol. Sci.* 34, DOI: 10.1002/pts.2554.

Mertoglu-Elmas, G. (2017). "The effect of colorants on the content of heavy metals in recycled corrugated board papers," *BioResources* 12(2), 2690-2698. DOI: 10.15376/biores.12.2.2690-2698

Norstrand, T. (2004). "On buckling loads for edge-loaded orthotropic plates including transverse shear," *Comp. Struct.* 65(1), 1-6. DOI: 10.1016/S0263-8223(03)00154-5

Park, J., Chang, S., and Jung, H. M. (2020). "Numerical prediction of equivalent mechanical properties of corrugated paperboard by 3D finite element analysis," *Appl. Sci*. 10(22), 7973. DOI: 10.3390/app10227973

Pozorska, J., and Pozorski Z. (2018). "The comparison of numerical models of a sandwich panel in the context of the core deformations at the supports," in: *AIP Conference Proceedings* 1922, article 050007, pp. 050007-1–050007-7. DOI: 10.1063/1.501906

Popil, R. E. (2012). "Overview of recent studies at IPST on corrugated board edge compression strength: Testing methods and effects of interflute buckling," *BioResources* 7(2), 2553-2581. DOI: 10.15376/biores.7.2.2553-2581

Putz, H.-J., and Schabel, S. (2018). "The myth of limited fibre life cycles," *Wochenblatt für Papierfabrikation* 6, 350-356.

Sapienza, V., Rodonò, G., Monteleone, A., and Calvagna, S. (2022). "ICARO - Innovative Cardboard ARchitecture Object: Sustainable building technology for multipurpose micro-architecture," *Sustainability* 14, article 16099. DOI: 10.3390/su142316099

Schrampfer, K. E., Whitsitt, W. J., and Baum, G. A. (1987). *Combined Board Edge Crush (ECT) Technology*, Institute of Paper Chemistry, Appleton, WI, USA.

Sohrabpour, V., and Hellström, D. (2011). "Models and software for corrugated board and box design," in: *Proceedings of the 18th International Conference on Engineering Design*, ICED 11, Copenhagen, Denmark.

Urbanik, T. J., and Saliklis, E. P. (2003). "Finite element corroboration of buckling phenomena observed in corrugated boxes," *Wood Fiber Sci.* 35(3), 322-333.

Urbanik, T. J., and Frank, B. (2006). "Box compression analysis of world-wide data spanning 46 years," *Wood Fiber Sci.* 38(3), 399-416.

Wang, C.-C., Chen, C.-H., and Jiang, B. C. (2021). "Shock absorption characteristics and optimal design of corrugated fiberboard using drop testing," *Appl. Sci*. 11, article 5815. DOI: 10.3390/app11135815

Yoshihara, H., Yoshinobu, M., and Maruta, M. (2022). "Bending stiffness and moment capacity of cardboard obtained from three-point and elastic bending tests," *Nordic Pulp & Paper Research Journal* 38, 1, 73-85. DOI: 10.1515/npprj-2022-0087

Article submitted: July 17, 2023; Peer review completed: August 26, 2023; Revised version received and accepted: September 14, 2023; Published: September 20, 2023.
DOI: 10.15376/biores.18.4.7611-7628